Modulation of Synaptic GABA_A Receptor Function by PKA and PKC in Adult Hippocampal Neurons

Pierrick Poisbeau,[2] Michael C. Cheney,[1] Michael D. Browning,[3] and Istvan Mody[1]

[1]*Departments of Neurology and Physiology, University of California at Los Angeles, School of Medicine, Los Angeles, California 90095,* [2]*Laboratoire de Neurophysiologie Cellulaire et Intégrée, Centre National de la Recherche Scientifique UMR 7519, Université Louis Pasteur, 67084 Strasbourg, France, and* [3]*Department of Pharmacology, University of Colorado Health Science Center, Denver, Colorado 80262*

Several protein kinases are known to phosphorylate Ser/Thr residues of certain GABA_A receptor subunits. Yet, the effect of phosphorylation on GABA_A receptor function in neurons remains controversial, and the functional consequences of phosphorylating synaptic GABA_A receptors of adult CNS neurons are poorly understood. We used whole-cell patch-clamp recordings of GABA_A receptor-mediated miniature IPSCs (mIPSCs) in CA1 pyramidal neurons and dentate gyrus granule cells (GCs) of adult rat hippocampal slices to determine the effects of cAMP-dependent protein kinase (PKA) and Ca^{2+}/phospholipid-dependent protein kinase (PKC) activation on the function of synaptic GABA_A receptors. The mIPSCs recorded in CA1 pyramidal cells and in GCs were differentially affected by PKA and PKC. In pyramidal cells, PKA reduced mIPSC amplitudes and enhanced the fraction of events decaying with a double exponential, whereas PKC was without effect. In contrast, in GCs PKA was ineffective, but PKC increased the peak amplitude of mIPSCs and also favored double exponential decays. Intracellular perfusion of the phosphatase inhibitor microcystin revealed that synaptic GABA_A receptors of pyramidal cells, but not those of GCs, are continually phosphorylated by PKA and conversely, dephosphorylated, most likely by phosphatase 1 or 2A. This differential, brain region-specific phosphorylation of GABA_A receptors may produce a wide dynamic range of inhibitory synaptic strength in these two regions of the hippocampal formation.

Key words: GABA_A; miniature IPSCs; phosphorylation; receptors; PKA; PKC

Phosphorylation of ligand-gated ion channels is an important short- and long-term regulatory mechanism of channel function in the CNS (Levitan, 1994; Sigel, 1995; Moss and Smart, 1996). In the process of long-term potentiation (LTP) of synaptic transmission, experimental evidence strongly supports a critical role of protein kinases (for review, see Raymond et al., 1993; Soderling, 1995; McEachern and Shaw, 1996; Barria et al., 1997). A recent study (Barria et al., 1997) has directly demonstrated the phosphorylation of AMPA-type glutamate receptors (GluRs) by type II Ca^{2+}/calmodulin kinase after LTP.

In contrast to the familiar plasticity of excitatory amino acid receptors through phosphorylation, fewer studies implicate this process in altering the efficacy of GABAergic synaptic transmission. In Purkinje cells, repetitive stimulation of climbing fibers induces a rebound potentiation of GABA_A receptor (GABAR) function (Kano et al., 1996). This potentiation has been attributed to elevated postsynaptic Ca^{2+} levels over 10–30 min, possibly leading to protein phosphorylation. Various cells when deprived of intracellular ATP by omitting it from the patch pipette commonly respond by downregulating GABAR function (Raymond et al., 1993; Sieghart, 1995; Moss and Smart, 1996). Most

studies examined whole-cell currents evoked by GABA in expression systems, but a rundown of GABAR-mediated synaptic currents has been noted in central neurons (Lewis and Faber, 1996).

Biochemical approaches demonstrated that some native and many recombinantly expressed GABARs can be phosphorylated directly and consequently can be functionally modulated by cAMP-dependent kinase (PKA) (Heuschneider and Schwartz, 1989; Tehrani et al., 1989; Browning et al., 1990; Porter et al., 1990; Leidenheimer et al., 1991; Moss et al., 1992a,b; Angelotti et al., 1993; Browning et al., 1993), Ca^{2+}/phospholipid-dependent protein kinase (PKC) (Sigel and Baur, 1988; Browning et al., 1990, 1993; Sigel et al., 1991; Leidenheimer et al., 1992; Krishek et al., 1994; Lin et al., 1994; Chang et al., 1996; Weiner et al., 1997), type II Ca^{2+}/calmodulin-dependent protein kinase (Machu et al., 1993; McDonald and Moss, 1994, 1997), or protein tyrosine kinase (Moss et al., 1995; Wan et al., 1997). In general, phosphorylation of Ser/Thr residues on GABAR subunits by PKC and PKA is believed to decrease GABAR function (Sigel, 1995; Moss and Smart, 1996), although some reports show an increase in GABA_A receptor-mediated whole-cell currents by PKC (Lin et al., 1994) and PKA (Cheun and Yeh, 1992; Angelotti et al., 1993; Cheun and Yeh, 1996). Tyrosine phosphorylation seems to be involved in either potentiating or maintaining GABAR-mediated inhibition (Moss et al., 1995; Wan et al., 1997; Huang and Dillon, 1998).

Unfortunately, the precise subunit composition of synaptic GABARs as well as the local enzymatic machinery are not known. Therefore, no accurate predictions can be made about the effect of phosphorylation on the modulation of GABAR-mediated synaptic transmission. With the exception of a recent

study showing altered IPSCs in cultured neurons after inhibition of the Ca^{2+}/CaM-dependent phosphatase calcineurin (Jones and Westbrook, 1997), there is no compelling evidence demonstrating the impact of phosphorylation on synaptic GABAR function.

We have investigated the postsynaptic effects of PKA and PKC in CA1 pyramidal cells and granule cells (GCs) of adult hippocampal slices using intracellular delivery of nonpermeant peptides and catalytic kinases. By recording mIPSCs in fully developed central neurons, we could focus on the modulation of synaptic GABAR function by PKA- and PKC-dependent phosphorylation.

MATERIALS AND METHODS

Slice preparation and solutions. Coronal slices were prepared from Wistar rats (350–400 gm) as described previously (Staley et al., 1992; Poisbeau et al., 1997). Briefly, after pentobarbital anesthesia (75 mg/kg, i.p.), animals were decapitated, and the brain was quickly removed and immersed for 1–2 min in cold (6–9°C) artificial CSF (ACSF) containing (in mM): 126 NaCl, 2.5 KCl, 2 $CaCl_2$, 2 $MgCl_2$, 1.25 NaH_2PO_4, 10 D-glucose, 26 $NaHCO_3$, 2 kynurenic acid (Fluka) continuously bubbled with 95% O_2/5% CO_2, pH 7.35 ± 0.05. The brain was glued at its frontal surface to a brass platform, and coronal brain slices (450 μm thick) were prepared with a Vibratome (Lancer Series 1000). The slices were then hemisected and stored submerged in 2 mM kynurenic acid containing ACSF at 32°C until they were individually transferred to the recording chamber. Recordings were performed at 34–35°C with slices immobilized with a piece of lens paper and two small platinum weights. During each recording, 1 μM tetrodotoxin (Calbiochem) was added to the ACSF in the continued presence of the nonspecific glutamate receptor antagonist kynurenic acid (2 mM).

With the exception of Rp-8-CPT-cAMPS, the compounds used to alter cellular phosphorylation events were membrane-impermeant peptides. PKC and PKA were isolated and purified from bovine brain as described previously (Browning et al., 1990). Only constitutively active catalytic subunits of these kinases were used. The catalytic subunit of PKA was purified from bovine heart as described previously (Browning et al., 1990). The catalytic fragment of PKC was prepared from bovine brain PKC as described previously (Wang et al., 1994). PKA-I (H_2N-TYADFIASGRTGRRNAI-amide) was a generous gift of Dr. John Haycock. PKA, PKC, inactivated PKC, PKA inhibitor, and microcystin have been diluted 50–1000 times when incorporated into the intracellular solution. Microcystin-LR (Calbiochem, La Jolla, CA) and Rp-8-CPT-cAMPS were first prepared as 1000-fold concentrated stock solutions in DMSO. PKA (0.3 mg/ml) and the PKA inhibitory peptide (PKA-I; 0.33 mM) were initially prepared in the following buffer solution (in mM): 100 NaCl, 20 MES, pH 6.5, 30 β-mercaptoethanol, 0.1 EDTA, and 50% ethylene glycol solution; PKC (0.3 mg/ml) was prepared in a solution consisting of the following (in mM): 2 TEA, 5 EGTA, 6 $MgCl_2$, 140 KCl, 1 $CaCl_2$, adjusted to pH 7.5 with KOH. An equivalent dilution of the buffer alone, when perfused into the cytoplasm of GC or CA1 neurons, did not produce any changes of GABA_A mIPSCs.

Whole-cell recordings and data collection. Whole-cell voltage-clamp recordings were obtained using borosilicate glass capillaries with an inner filament (KG-33, 1.12 mm inner diameter, 1.5 mm outer diameter; Garner Glass) pulled to tip diameters of ∼1.5 μm in two stages using a vertical puller (Narishige PP-83). Intrapipette solutions contained the following (in mM): 130 CsCl, 2 $MgCl_2$, 10 HEPES, 0.8 CsOH, 2 MgATP (pH was adjusted with CsOH; total osmolarity 255–285 mOsm). Recordings were obtained by lowering patch electrodes into the CA1 and/or dentate granule cell layer while monitoring current responses to 5 mV voltage pulses and applying suction to form >GΩ seals. An Axopatch-200A amplifier (Axon Instruments) was used, and series resistance (R_s) was compensated by 70–90% (lag value, 7–10 μsec). The value of R_s was monitored throughout each experiment, and only recordings with R_s < 15 MΩ lasting >20 min were considered acceptable for analysis. Recorded membrane currents were filtered (DC to 10 kHz, Bessel filter of the amplifier), digitized in a pulse-code-modulated form (88 kHz; Neurocorder, Neurodata), and stored on videotape. Off-line, recordings were filtered (DC to 3 kHz; −3 dB, eight-pole Bessel filter; Frequency Devices 9002) and sampled at 20 kHz on an Intel–Pentium-based computer. Data were acquired and analyzed using the Strathclyde Electrophysiology software (courtesy of Dr. J. Dempster, U. of Strathclyde, Glasgow, UK) and our own software designed by Y. De Koninck and I. Mody.

Event detection and selection. Detection of individual mIPSCs was

performed using a software trigger described previously in detail (Otis and Mody, 1992; Soltesz et al., 1995). More than 95% of events that satisfied the trigger criteria were detected, even during compound mIPSCs. For each experiment, all detected events were examined, and any spurious noise that triggered the detector was rejected.

Statistical analyses and curve fitting. The mean values of the median conductances, decay time constants, and frequencies of mIPSC occurrence were compared between groups using ANOVA. Decay time constants of mIPSCs were fitted using a simplex-based nonlinear least square method; goodness of fit was evaluated on the basis of fitting subsets of points drawn from the whole set of data points, from evaluation of the reduced χ^2 values, and from the change in the F values calculated by dividing the percentage reduction in the sum of squares by the percentage change in the number of degrees of freedom used for fitting (Soltesz and Mody, 1995; Williams et al., 1998). The conductance of mIPSCs is represented graphically in cumulative probability plots drawn on a probability scale ordinate. All numerical data are expressed as mean ± SD.

Simulation of mIPSCs. Simulations of mIPSCs were performed using the SCoP software (Simulation Resources, Berrien Springs, MI) according to a model based on that published by Jones and Westbrook (1995). For monoexponentially decaying mIPSCs, the model included two equal and independent GABA-binding steps, and a double-liganded open state. The maximum open probability at the peak of IPSCs (P_{MAX}) was taken to be 0.8–0.85 (Auger and Marty, 1997), a value similar to that derived by nonstationary noise analysis at hippocampal inhibitory synapses (De Koninck and Mody, 1994). The reported parameters represent the values producing the best fits to the experimental data.

RESULTS

Characteristics of GABAR-mediated mIPSCs in CA1 pyramidal cells and GCs

GABAR-mediated mIPSCs were recorded from CA1 neurons and GCs with CsCl-containing electrodes ($E_{Cl} = 0$ mV) at holding potentials around −60 mV in the presence of kynurenic acid (2 mM) and tetrodotoxin (1 μM).

Under these recording conditions, mIPSCs of CA1 neurons had fast rise times (10–90% rise time <0.8 msec) and predominantly monoexponential decays (Table 1, Fig. 1). However, a subpopulation of mIPSCs (∼6%) was better fit by a biexponential decay function (Table 1). This fraction of biexponentially decaying mIPSCs was not significantly changed in CA1 neurons in recordings with CsMeSO_4-containing electrodes ($E_{Cl} \cong -55$ mV) at a holding potential around 0 mV ($n = 8$; data not shown). The fast component (fast decay time constant, $\tau_{BIEXP\ FAST}$) accounted for 40% of the mIPSC amplitude. At negative holding potentials (−60 mV), mIPSC amplitudes ranged between 10 and 150 pA, with a mean conductance (mIPSG) of 0.79 ± 0.08 nS ($n = 19$). Because the mIPSG histograms were skewed [data not shown, but see Otis and Mody (1992)], we used the median values of the distributions obtained from the cumulative probability graphs (Table 1). No correlations were found between the 10–90% rise times, decay time constants (monoexponential, biexponential fast or slow), and mIPSC amplitudes. Biexponentially and monoexponentially decaying mIPSCs had similar median amplitudes and total areas. The frequency of GABAR-mediated mIPSCs was ∼20 Hz (Table 1). GABAR-mediated mIPSCs recorded from GCs displayed similar kinetics (Table 2, Fig. 2) but occurred with a significantly lower frequency (∼10 Hz) (Table 2).

Intracellular PKA reduces the amplitude of mIPSCs in CA1 neurons

We first compared mIPSC properties between CA1 neurons recorded with different intracellular solutions: mIPSCs recorded in cells with control solutions were compared with events recorded when the patch pipette was filled with similar solutions also containing constitutively active PKA or PKC. Intracellular PKA (0.6 or 6 μgm/ml) in CA1 neurons produced a dose-

Table 1. Summary of mIPSC characteristics recorded in CA1 pyramidal cells (indicated by *n* in each case) after intracellular perfusion of PKA, PKC, microcystin, and PKA-I peptide

CA1 pyramidal cells	Control	Boiled PKA (6 µg/ml)	Low PKA (0.6 µg/ml)	High PKA (6 µg/ml)	PKC (0.6–6 µg/ml)	Microcystin (20 µM)	Microcystin + high PKA	PKA-I (0.66 µM)	Microcystin + PKA-I
Conductance (nS)	0.72 ± 0.17	0.70 ± 0.11	**0.58 ± 0.14†**	**0.43 ± 0.05†**	0.71 ± 0.07	**0.49 ± 0.10†**	**0.51 ± 0.09†**	0.69 ± 0.10	0.67 ± 0.03
Frequency (Hz)	21.8 ± 6.8	20.8 ± 3.2	21.9 ± 8.6	22.8 ± 4.5	24.9 ± 5.3	24.7 ± 6.7	24.6 ± 3.5	25.3 ± 7.8	**37.4 ± 13.3†**
10–90% Rise time (msec)	0.69 ± 0.21	0.64 ± 0.03	0.67 ± 0.14	0.60 ± 0.12	0.60 ± 0.08	**0.56 ± 0.06†**	0.65 ± 0.07	0.65 ± 0.13	0.72 ± 0.10
τ_{MONOEXP} (msec)	3.82 ± 0.73	3.81 ± 0.17	3.66 ± 0.48	3.56 ± 0.64	3.79 ± 0.25	3.90 ± 0.33	3.77 ± 0.40	3.55 ± 0.27	3.61 ± 0.19
$\tau_{\text{BIEXP FAST}}$ (msec)	0.69 ± 0.36	0.67 ± 0.28	0.67 ± 0.24	0.69 ± 0.23	0.54 ± 0.16	0.63 ± 0.20	0.63 ± 0.43	0.69 ± 0.21	0.64 ± 0.19
$\tau_{\text{BIEXP SLOW}}$ (msec)	4.86 ± 1.17	4.68 ± 0.61	4.52 ± 0.55	4.56 ± 0.67	4.46 ± 0.42	5.22 ± 0.82	4.38 ± 1.09	4.85 ± 0.44	4.53 ± 0.60
BIEXPONENTIAL/TOTAL (%)	6.8 ± 3.9	5.6 ± 2.8	**17.8 ± 5.5†**	**20.5 ± 4.4†**	6.0 ± 1.7	**24.7 ± 10.0†**	**23.0 ± 8.3†**	12.5 ± 5.7	7.6 ± 5.0
	n = 19	*n* = 6	*n* = 8	*n* = 6	*n* = 10	*n* = 12	*n* = 5	*n* = 8	*n* = 5

The table depicts mIPSC conductance, frequency, 10–90% rise time, monoexponential decay time constant (τ_{MONOEXP}), biexponential fast ($\tau_{\text{BIEXP FAST}}$) and slow ($\tau_{\text{BIEXP SLOW}}$) decay time constants, and the fraction of biexponentially decaying mIPSCs from the total number of mIPSCs (BIEXPONENTIAL/TOTAL). Values in bold (also marked with †) are significantly different from the control (ANOVA, $p < 0.05$). Significant decreases in mIPSC conductances were found in the presence of PKA (0.6–6 µg/ml) and/or microcystin (20 µM). The inhibition of mIPSCs was always correlated with an increase in the fraction of biexponentially decaying currents. Boiled PKA, PKC, or PKA-I parameters were similar to the control. The microcystin-associated reduction of mIPSC conductance was prevented by coapplication of PKA-I.

dependent decrease of mIPSC conductance (−19.8 and −39.6%, respectively) (Table 1, Fig. 1), as well as a threefold increase in the fraction of biexponentially decaying mIPSCs. The reduction in amplitude affected the whole population of mIPSCs as shown in Figure 1*B* (*left panel*), where a parallel shift of the amplitude distribution is evident. No changes in mIPSC kinetics (rise time, decay) or frequency (Fig. 1*B*, *right panel*) were detected (Table 1).

The properties of mIPSCs in CA1 neurons were unaltered by inclusion of PKC (0.6 or 6 µgm/ml) in the patch pipette (Table 1, Fig. 1). This did not stem from the ineffectiveness of the perfused PKC, because we regularly observed a progressive reduction of the holding current during the first 5 min of recordings with PKC in the electrode (data not shown; *n* = 8). This was never seen in control recordings or during perfusion with inactive PKC (*n* = 4). The change in the holding current most likely results from the effect of PKC on the hyperpolarization-activated Cl$^-$ current through ClC2 channels known to be present in CA1 pyramidal cells (Smith et al., 1995). This was further corroborated by our finding that in recordings with CsMeSO$_4$ in the pipette (*n* = 7; $E_{\text{Cl}} \cong -56$ mV), at positive holding potentials (+20 mV) where there should be no ClC2 current (Smith et al., 1995), PKC did not alter the holding current and had no effect on mIPSCs.

Intracellular PKC increases the amplitude of mIPSCs in dentate gyrus granule cells

Using the same protocol as for CA1 pyramidal cells, we compared the effects of intracellular PKA and PKC on mIPSCs recorded in GCs. PKC (0.6 or 6 µgm/ml) increased mIPSG by 13.6% without affecting mIPSC frequency, 10–90% rise time, or decay time constants (Table 2, Fig. 2). As shown in Figure 2*B*, the increase of mIPSC amplitude only occurred in a subset (60–80%) of the total population of mIPSCs with a conductance >0.5 nS (Fig. 2*B*, *left panel*). We also observed a fourfold increase in the proportion of biexponentially decaying mIPSCs (Table 2, Fig. 2*C*). In GCs perfused with heat-inactivated PKC (*n* = 4), mIPSCs had characteristics similar to those found in control neurons. PKA (6 µgm/ml) failed to have any effect on the mIPSC recorded in GCs (Table 2, Fig. 2).

Simulations of the effects of phosphorylation on GABAR-mediated mIPSCs

GABAR-mediated mIPSCs were simulated according to a seven-state model (Macdonald and Olsen, 1994; Jones and Westbrook,

1995). We found the simplest model to accurately describe the experimentally observed mainly monoexponentially decaying mIPSCs to be a subset of four states of the original model (Fig. 3). The inclusion of an additional open state was sufficient to describe the biexponentially decaying mIPSCs. Additional desensitized states (Jones and Westbrook, 1995) did not substantially improve the fit of our simulations to the experimental data. We next compared the fitted parameters for simulated CA1 mIPSCs during PKA dialysis and control conditions. Although the fits are by no means unique, certain trends in the values of the rate constants (see Table in Fig. 3) are consistent with previously reported PKA effects on GABARs. For example, single-channel studies from spinal neurons have shown that PKA decreases the mean open time, increases the mean closed time, and decreases open probability (Porter et al., 1990). Our model shows at least a qualitative agreement with the increase in mean closed time (1/β2; Table in Fig. 3) and a decrease in maximum open probability at peak (from 0.85 to 0.50). The accurate simulation of the PKA effect also required the GABA binding rate to be altered. This may be warranted in light of the possible effect of phosphorylation on GABA potency, corresponding to a change in binding and unbinding rates (Porter et al., 1990).

Continuous regulation of synaptic GABAR function by phosphorylation/dephosphorylation in CA1 neurons

Intracellular perfusion of protein kinases and their constitutively active derivatives is useful to establish whether phosphorylation by the given kinase has any effect on cellular functions. However, a positive finding with a kinase does not necessarily prove the involvement of the given kinase in the physiological regulation of channel function. A positive effect of a phosphatase inhibitor is a more convincing and unequivocal evidence for the physiological involvement of the phosphorylation/dephosphorylation process. If inhibition of the phosphatase significantly affects receptor function, the most plausible conclusion is that under basal conditions a kinase must mediate the phosphorylation of at least one of the proteins involved. To determine this possibility in the phosphorylation-dependent regulation of synaptic GABARs, we next examined the effects of microcystin (20 µM), an inhibitor of protein phosphatases 1 and 2A (PP$_{1/2A}$). In CA1 pyramidal cells, inclusion of microcystin in the patch pipette gradually reduced mIPSC median conductance (−33.1%) in a manner analogous to
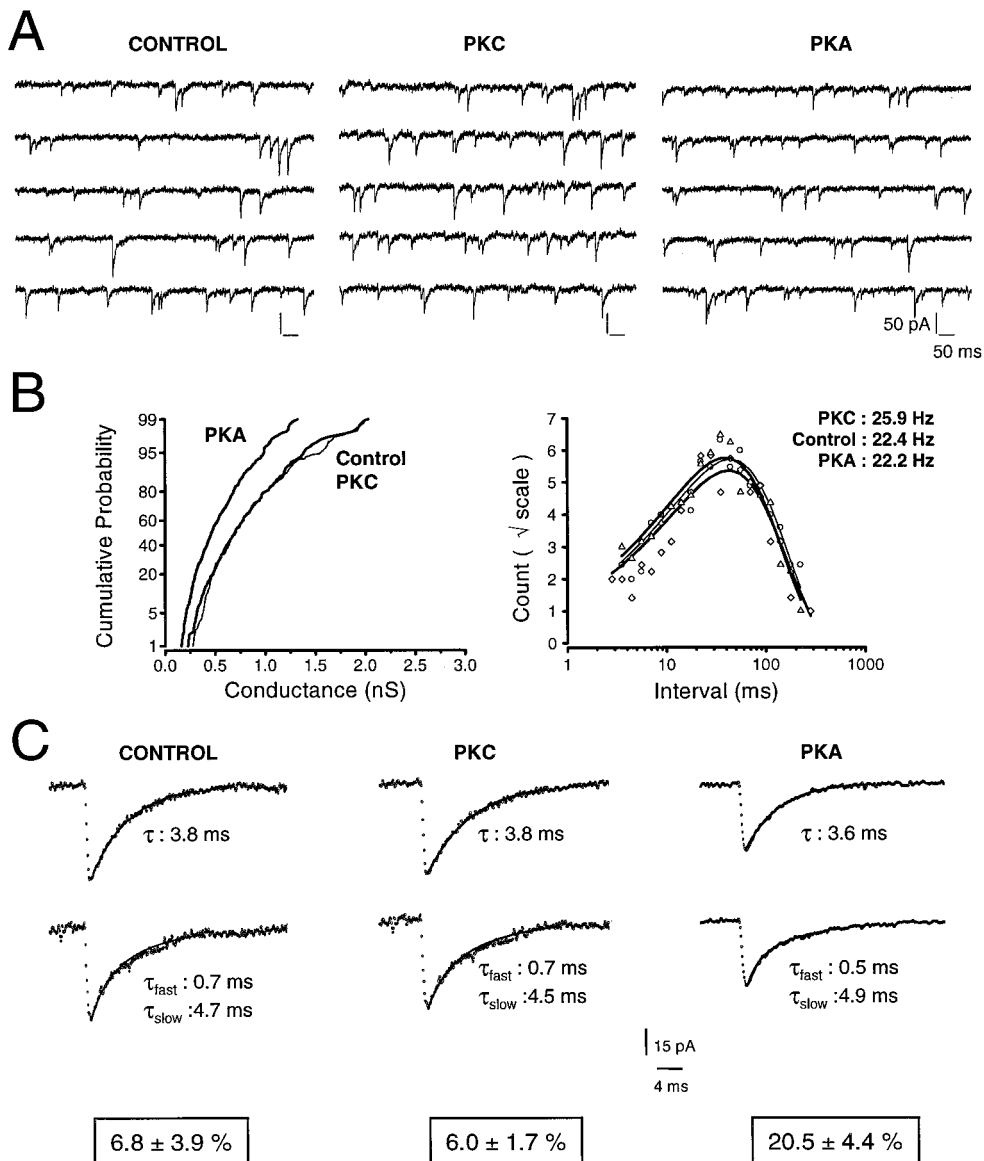
CA1 Pyramidal Cells

A

CONTROL **PKC** **PKA**

50 pA

50 ms

B

PKA

Control
PKC

Cumulative Probability

Conductance (nS)

Count (√ scale)

Interval (ms)

PKC : 25.9 Hz
Control : 22.4 Hz
PKA : 22.2 Hz

C

CONTROL **PKC** **PKA**

τ : 3.8 ms τ : 3.8 ms τ : 3.6 ms

τ_{fast} : 0.7 ms τ_{fast} : 0.7 ms τ_{fast} : 0.5 ms
τ_{slow} :4.7 ms τ_{slow} :4.5 ms τ_{slow} :4.9 ms

15 pA

4 ms

6.8 ± 3.9 % 6.0 ± 1.7 % 20.5 ± 4.4 %

Figure 1. Effects of protein kinase A (*PKA*) and protein kinase C (*PKC*) on mIPSCs recorded in CA1 pyramidal cells. *A*, Representative recordings (2.5 sec in total) depicting mIPSCs recorded with control intracellular solutions (*left*) and with 6 μgm/ml PKC (*middle*) or 6 μgm/ml PKA (*right*) in the patch pipette. Note the reduced mIPSCs amplitudes in the presence of PKA. *B*, The *left panel* shows cumulative probability distributions of mIPSC peak conductances under the three different experimental conditions. Compared with control (*thin line*; n = 393 mIPSCs), PKA (*thick line*; n = 525 mIPSCs) shifted the conductance distribution to the left in a roughly parallel manner, indicating a reduction in mIPSCs amplitude. PKC (*thick line*; n = 278 mIPSCs) had no significant effect compared with control. *Right panel* represents log-binned (10 bins/decade) interevent intervals plotted on a square root ordinate. The mean frequency in control (*circles*; n = 393 mIPSCs) was 22.4 Hz, compared with 22.2 Hz with intracellular PKA (*triangles*; n = 525 mIPSCs) and 25.9 Hz with intracellular PKC (*diamonds*; n = 278 mIPSCs). Fitted lines are fitted exponential probability density functions illustrating the random occurrence of mIPSCs. *C*, Representative examples of monoexponentially and biexponentially decaying mIPSCs. Each trace represents an average of 25 mIPSCs. The decay time constants were unaltered after dialysis of PKC. However, intracellular perfusion of PKA produced a significant increase in the fraction of biexponentially decaying mIPSCs (20.6 ± 4.8%) compared with control (5.9 ± 0.5%) or PKC (5.8 ± 1.8%).

that seen with PKA perfusion (Table 1, Fig. 4*A*). A 3.6-fold increase in the fraction of biexponentially decaying mIPSCs was also observed (Table 1). No other changes in CA1 pyramidal cell mIPSC parameters or their frequency were observed when microcystin was present in the intracellular solution (Table 1).

In GCs, microcystin (20 μM) did not change the mIPSG (Table 2, Fig. 4*B*) but caused a 1.8-fold increase in the fraction of biexponentially decaying mIPSCs (Table 2). As in CA1 neurons, mIPSC 10–90% rise times and frequency of occurrence were unaffected by microcystin (Table 2).

The time course of PKC, PKA, and microcystin effects on mIPSCs

Figure 4*C* displays the time-dependent changes in mIPSG recorded in CA1 pyramidal cells and GCs in the presence of control intracellular solutions, PKC, PKA, or microcystin. In control whole-cell recordings, the median mIPSG remained stable, but in CA1 neurons, PKA (6 μgm/ml) and microcystin (20 μM) decreased mIPSG during whole-cell recordings in a time-dependent

manner, whereas in GCs only PKC (6 μgm/ml) had a gradual, time-dependent effect on mIPSG. As indicated in the figure, significant effects were seen after 6–7 min and after 9–10 min of whole-cell recordings in the presence of PKA in CA1 cells and PKC in the GCs, respectively

Endogenous PKA is responsible for the microcystin-induced reduction of mIPSC amplitudes in CA1 pyramidal cells

To ascertain whether PKA was the endogenous protein kinase involved in the regulation of mIPSCs in CA1 pyramidal cells, we suppressed endogenous phosphatase activity by microcystin and simultaneously reduced the activity of protein kinase A. Specific inhibitors of PKA (PKA-I, 0.66 μM included in the patch electrode; and Rp-8CPT-cAMP-S, 100 μM perfused extracellularly) were applied with or without intracellular microcystin (20 μM). According to an *in vitro* biochemical assay, the intrapipette concentration of PKA-I was sufficient to inhibit 15 μgm/ml of PKA (M. D. Browning, unpublished observations). The microcystin-

Table 2. Summary of mIPSC characteristics recorded in GCs (indicated by *n* in each case) after intracellular perfusion of PKA, PKC, and microcystin

Dentate gyrus granule cells	Control	Inactive PKC (6 μg/ml)	PKC (0.6–6 μg/ml)	PKA (6 μg/ml)	Microcystin (20 μM)
Conductance (nS)	0.67 ± 0.08	0.68 ± 0.05	**0.76 ± 0.07†**	0.66 ± 0.12	0.69 ± 0.13
Frequency (Hz)	10.9 ± 5.3	11.2 ± 2.4	11.8 ± 3.1	11.5 ± 3.5	10.9 ± 3.9
10–90% Rise time (msec)	0.67 ± 0.14	0.66 ± 0.03	0.63 ± 0.09	0.60 ± 0.08	**0.55 ± 0.05†**
τ_{MONOEXP} (msec)	3.83 ± 0.41	3.89 ± 0.36	3.75 ± 0.29	3.83 ± 0.28	3.76 ± 0.35
$\tau_{\text{BIEXP FAST}}$ (msec)	0.73 ± 0.21	0.74 ± 0.08	0.73 ± 0.13	0.72 ± 0.19	0.71 ± 0.21
$\tau_{\text{BIEXP SLOW}}$ (msec)	4.73 ± 0.75	4.86 ± 0.12	4.56 ± 0.87	4.81 ± 0.45	4.99 ± 0.78
BIEXPONENTIAL/TOTAL (%)	5.9 ± 1.6	6.2 ± 1.2	**22.9 ± 6.8†**	6.0 ± 3.9†	**15.2 ± 8.3†**
	n = 11	*n* = 4	*n* = 11	*n* = 7	*n* = 8

The table shows the mIPSC conductance, frequency, 10–90% rise time, monoexponential decay time constant (τ_{MONOEXP}), biexponential fast ($\tau_{\text{BIEXP FAST}}$) and slow ($\tau_{\text{BIEXP SLOW}}$) decay time constants, and the fraction of biexponentially decaying mIPSCs from the total number of mIPSCs (BIEXPONENTIAL/TOTAL). Values in bold (also marked by †) are significantly different from the control (ANOVA, $p < 0.05$). Significant increases in mIPSC conductances were found in the presence of PKC (0.6–6 μg/ml). Except for an increase in the fraction of bi-exponentially decaying current in the presence of microcystin, no changes were noted in any of the other treatments.

associated reduction in mIPSG was completely antagonized by inclusion of PKA-I in the electrode or by perfusion of Rp-8-CPT-cAMP-S (Table 1, Fig. 5). Although Rp-8-CPT-cAMP-S is cell-permeant, it produced no apparent presynaptic changes as seen by the constant frequency of mIPSCs. In all of these experiments the mIPSC kinetics remained comparable to those observed in control recordings or in cells with boiled PKA in the electrode (Table 1). It is interesting to note that inclusion of active PKA together with the phosphatase inhibitor produced no additive effects on mIPSCs (Fig. 5). This may mean that the rate of dephosphorylation is most likely the rate-limiting step in the control of synaptic GABAR function.

DISCUSSION

We have studied the regulation of GABAR-mediated mIPSCs by protein kinases and phosphatases. Our results are consistent with the involvement of PKA and PKC in the regulation of synaptic GABAR function in CA1 pyramidal cells and GCs, respectively. There were remarkable differences, however, between the phosphorylation-dependent modulation of mIPSCs in the two cell types. Activation of PKA alters synaptic GABAR function only in CA1 pyramidal cells, whereas PKC changes mIPSCs recorded in GCs. Moreover, PKA decreased mIPSC amplitudes in CA1 pyramidal cells, whereas PKC increased mIPSC amplitudes in GCs. The 10–90% rise and decay time constants of mIPSCs in both CA1 and GCs were unaffected by intracellular kinase administration. Both kinases produced an increase in the fraction of biexponentially decaying mIPSCs. The results with intracellular microcystin, a PP$_{1/2A}$ inhibitor, are consistent with endogenous PKA being steadily active in CA1 neurons but not in GCs. Thus, the net balance between phosphorylation and dephosphorylation will critically alter the strength of GABA$_A$ synapses.

Specificity of the phosphorylation effect to synaptic GABARs

In acute or cultured hippocampal slices, membrane-permeable activators of PKC and PKA dramatically increase the frequency of mIPSCs recorded in CA1 and CA3 pyramidal cells (Pitler and Alger, 1994; Aniksztejn et al., 1995; Capogna et al., 1995), without altering mIPSC amplitudes. However, any possible postsynaptic effect of the membrane-permeable compounds might have been obscured by the powerful presynaptic action. In our studies, the direct intracellular administration of membrane-impermeable compounds such as microcystin or constitutively active PKC and

PKA was designed to eliminate interference with presynaptic mechanisms, thus allowing us to strictly monitor the postsynaptic regulation of synaptic GABARs. Some of our findings, such as the lack of PKC effect on GABAR-mediated mIPSC amplitude in CA1, are in agreement with previous studies reporting purely presynaptic effects of extracellularly applied PKC activators (Pitler and Alger, 1994). Nevertheless, it is possible that the lack of effect of PKC in the CA1 region could be caused by our failure to apply the correct PKC isotype. We consider this possibility unlikely because our PKC preparation contains three isoforms (α, β, and γ), and the various isoforms do not appear to have unique substrates, only some differences in the kinetics of phosphorylation (Kazanietz et al., 1993).

Despite the purely postsynaptic route of administration of active compounds, we have observed effects on mIPSC frequency that might be interpreted as being of presynaptic origin. For example, when the PP$_{1/2A}$ inhibitor microcystin was coadministered with PKA-I, there was a significant 50% increase in the frequency of mIPSCs without any significant change in their amplitudes. If this effect is indeed presynaptic, one possibility is that the simultaneous inhibition of PKA and of PP$_{1/2A}$ may have released a transsynaptic messenger that leads to an enhanced GABA release or to a reduced tonic inhibitory effect on the presynaptic terminals. A transsynaptic modulation of GABA release is believed to occur through release of glutamate onto presynaptic metabotropic glutamate receptors (Glitsch et al., 1996), most likely belonging to group I (Morishita et al., 1998). Alternatively, the observed increase in mIPSC frequency may be entirely of postsynaptic origin. If one assumes that GABA$_A$ synapses can be kept "silent" (Poisbeau et al., 1997), the simultaneous inhibition of PKA and PP$_{1/2}$ may produce a conversion of silent synapses into active ones. Then, if the unitary events generated at these synapses are similar to mIPSCs recorded under control conditions, the "uncovered" events would be indistinguishable from controls and would simply add to existing mIPSCs producing the increase in frequency. At present, there are no data to support either possibility.

The GABAR subunit as a possible target of phosphorylation

With the exception of their frequency of occurrence, there are remarkable similarities between mIPSCs recorded in CA1 pyramidal cells and GCs. It is therefore puzzling to find such different actions of PKA and PKC on the function of synaptic GABARs.
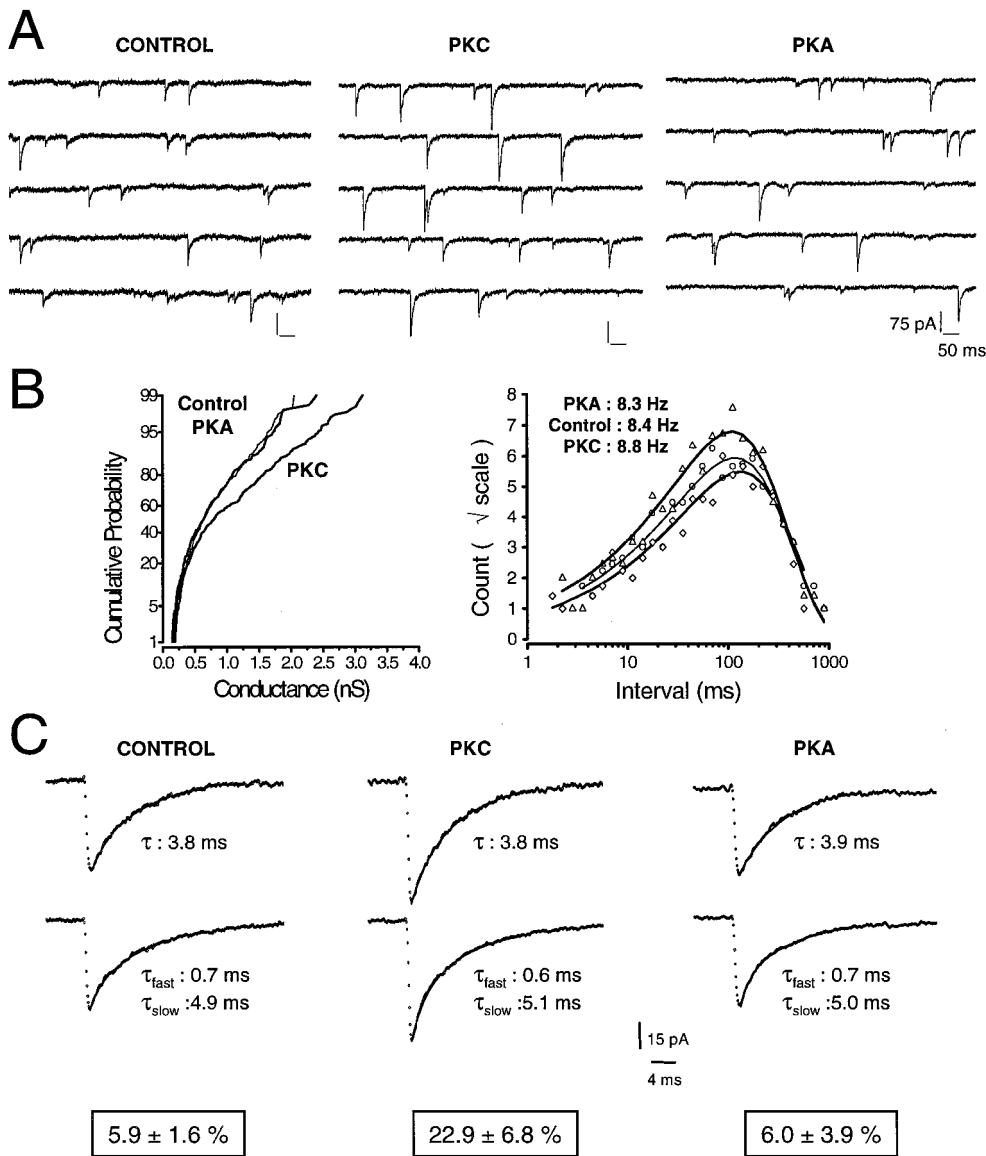
Dentate Gyrus Granule Cells

Figure 2. Effects of protein kinase A (*PKA*) and protein kinase C (*PKC*) on mIPSCs recorded in dentate gyrus granule cells. *A*, Raw traces (2.5 sec in total) of mIPSCs recorded with control intracellular solutions (*left*) and with solutions containing 6 μgm/ml PKC (*middle*) or 6 μgm/ml PKA (*right*) in the patch pipettes. Note the increased incidence of large amplitude mIPSCs in the recording with a PKC-containing pipette. *B*, The *left panel* shows the cumulative probability distribution of mIPSC peak conductances. The effect of PKA on the conductance distribution (*thick left trace*; $n = 245$ mIPSCs) is not significantly different from control (*thin trace*; $n = 324$ mIPSCs). PKC (*thick right trace*; $n = 403$ mIPSCs) elicited a marked increase in larger amplitude mIPSCs compared with control. *Right panel* shows log-binned (10 bins/decade) interevent intervals plotted on a square root ordinate. The mean frequency of mIPSCs under control conditions was 8.4 Hz (*circles*; $n = 324$ mIPSCs), compared with 8.3 Hz with PKA (*triangles*; $n = 245$ mIPSCs) and 8.8 Hz with PKC (*diamonds*; $n = 403$ mIPSCs) in the pipette. Fitted lines are exponential probability density functions illustrating the random nature of mIPSCs. *C*, Illustration of monoexponentially (*top left, middle,* and *right traces*) and biexponentially decaying mIPSCs (*lower left, middle,* and *right traces*). Each trace is an average of 25 mIPSCs. In the presence of PKC and PKA, the single or double exponential decay time constants were similar to control values. However, PKC was found to increase the fraction of biexponentially decaying mIPSCs to 24.4 ± 7.8% of total, compared with control (5.2 ± 0.9% of total) or intracellular PKA conditions (6.8 ± 3.3% of total).

If a direct phosphorylation of GABAR subunits is involved in the effects seen in our study, a different subunit composition of the receptors in the two regions might explain the observed differences in their phosphorylation-dependent regulation. Albeit minor, there are some divergences in the molecular identities of GABARs present in the two cell types. For example, GCs express δ and $\alpha 4$ subunits, whereas $\alpha 5$ subunits are mostly found in CA1 pyramidal cells. Most other subunits are shared by the two populations. Accordingly, the presence of specific subunits in synaptic GABAR aggregates may be responsible for the region specificity as well as for the direction of the alterations induced by phosphorylation. In this context, however, it is interesting to note that to date there are no reports about differential effects of phosphorylation on $\alpha 4$ and $\alpha 5$ subunits, and possible effects of phosphorylating δ subunits may be discounted, because at least in the cerebellum, δ subunit-containing receptors are found exclusively extrasynaptically (Jones et al., 1997; Nusser et al., 1998).

Our experiments do not allow us to reach conclusions about a *direct* phosphorylation of GABARs by PKA or PKC. However, the simplest explanation supported by strong experimental evidence is that specific GABAR subunits can be phosphorylated and that this phosphorylation modifies GABAR function (Levitan, 1994; Macdonald and Olsen, 1994; Sieghart, 1995; Sigel, 1995; Moss and Smart, 1996). It appears that β subunits are the best substrates for PKA- and PKC-dependent phosphorylation, but unequivocal conclusions are complicated by the fact that β subunits are not the sole potential targets for phosphorylation (Macdonald and Olsen, 1994). Mutagenesis of Ser409 of the $\beta 1$ subunit eliminates PKA-induced regulation of GABAR function (Moss et al., 1992a,b). A recent report (McDonald et al., 1998) has further characterized the differential effects of PKA-dependent phosphorylation of β subunit-containing recombinant GABARs. It appears that $\beta 2$ subunit-containing receptors, which should be the most predominant β subunits in hippocampal neurons (McKernan and Whiting, 1996), are not affected by PKA-dependent phosphorylation. The phosphorylation of $\beta 1$ subunits reduces the
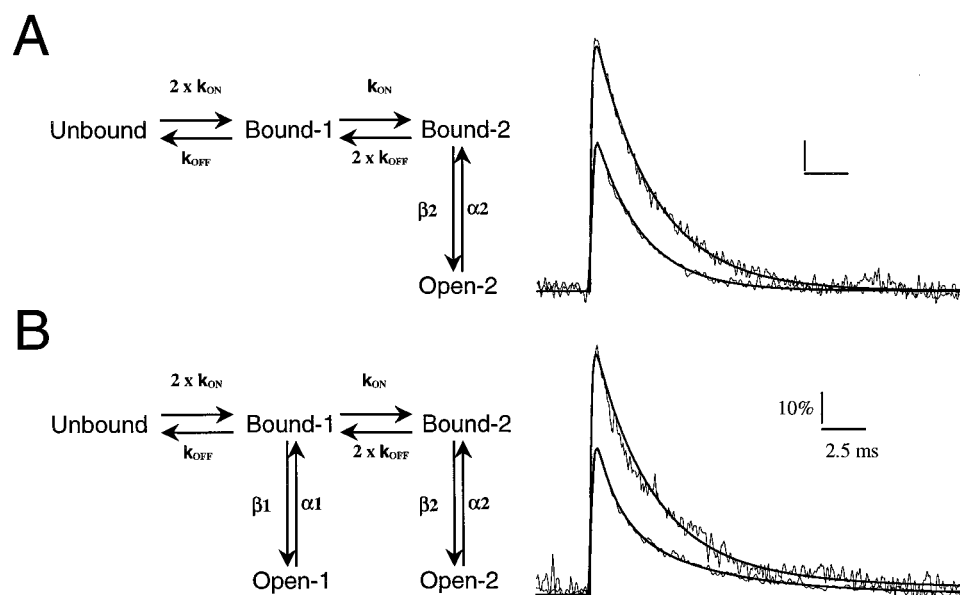
Figure 3. Modeling of monoexponentially and biexponentially decaying mIPSCs. Monoexponentially (*A*) and biexponentially (*B*) decaying events were simulated using the models depicted in the *left panels* (one or two open state). *Right panels* show the results of simulations with the fitted curves superimposed over the averages of 25 mIPSCs. The *y*-axis represents open probability, with data normalized to a p_{open} of 0.85 at the peak of the mIPSC. The table gives the parameters used to simulate the various events.

Constant	Control		PKA	
	Mono-exponential	Bi-exponential	Mono-exponential	Bi-exponential
k_{ON} (M^{-1}s^{-1})	2.26×10^8	2.26×10^8	6.24×10^5	1.02×10^6
k_{OFF} (s^{-1})	950	950	2000	1600
$\beta1$ (s^{-1})	0	55	0	356
$\alpha1$ (s^{-1})	0	44	0	215
$\beta2$ (s^{-1})	12111	12111	7500	4617
$\alpha2$ (s^{-1})	2437	2437	1120	2172
Duration of GABA Pulse (ms)	0.4	0.4	0.4	0.4
[GABA] (mM)	10	10	10	10

current flow through recombinant GABARs, whereas the same process on $\beta3$ subunit-containing receptors produces the opposite effect. If the effect of PKA on mIPSCs stems indeed from phosphorylation of β subunits, the β subunit selectivity of the PKA-dependent phosphorylation may indicate that GABARs at synapses of CA1 pyramidal cells preferentially contain $\beta1$ subunits, whereas those at inhibitory synapses on GCs contain mainly $\beta2$ subunits.

As mentioned above, our findings do not necessarily demonstrate a *direct* phosphorylation of a given GABAR subunit. Indeed, phosphorylation of a GABAR-associated protein that controls its function may be responsible for the regional differences observed in our study. Such proteins have yet to be conclusively demonstrated at GABA$_A$ synapses, but there is ample evidence from glutamate synapses that such proteins can be closely associated with synaptic receptors (Kennedy, 1997; Sheng and Wyszynski, 1997). Regardless of the exact mechanism for the disparate regulation of synaptic GABARs in CA1 pyramidal cells and GCs, there is a noteworthy similarity between our present findings and the differential effect of withdrawal from chronic benzodiazepine treatment in these two types of neuron (Poisbeau et al., 1997). The mIPSCs of GCs are insensitive to *in vivo* benzodiazepine withdrawal, whereas the size of mIPSCs recorded in CA1 pyramidal neurons significantly decreases during the with-

drawal period. Whether there is a relationship between the sensitivity of synaptic GABARs to PKA-dependent phosphorylation reported in the present study and the effects of long-term benzodiazepine treatment on these receptors remain to be determined.

Continuous PKA-dependent phosphorylation in CA1 pyramidal cells

We have shown a continuous cycle of a PKA-dependent phosphorylation and a PP$_{1/2A}$-dependent dephosphorylation to affect the function of synaptic GABARs in CA1 pyramidal cells. It is tempting to speculate that the small fraction of mIPSCs with a double exponential decay might be the result of such continuous phosphorylation. However, the proportion of such events was unaffected by inhibition of PKA. Such a basal phosphorylation/dephosphorylation cycle does not seem to alter the function of GABARs at synapses in GCs, although activation of the PKC pathway could induce an increase in mIPSC amplitude. In CA1 pyramidal cells, promoting phosphorylation will inhibit synaptic GABARs, whereas tipping the balance in favor of dephosphorylation will enhance inhibitory events. Thus, dephosphorylation of the GABARs, or of closely associated proteins, by PP$_{1/2A}$ can play a crucial role in regulating inhibitory strength in CA1 pyramidal cells. In addition, calcium-dependent phosphatases and kinases

A   CA1 Pyramidal Cells
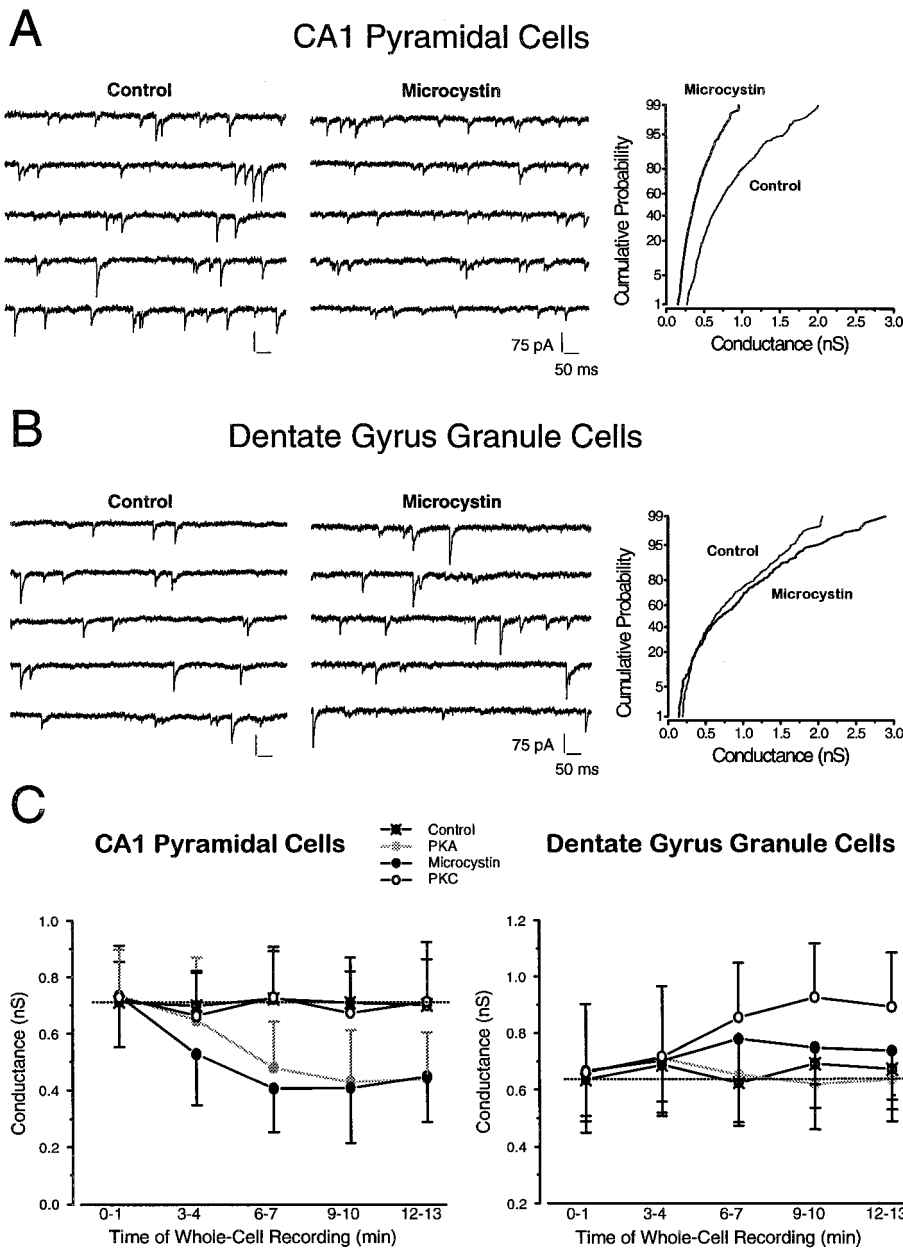
Control   **Microcystin**

75 pA | 50 ms

Figure 4. A, B, Effect of microcystin on mIPSCs recorded from dentate gyrus GCs and CA1 pyramidal cells. *Left panels* show five consecutive raw traces (500 msec each, i.e., 2.5 sec in total) from a CA1 pyramidal cell (*A*) and a dentate gyrus GC (*B*). The *middle panels* show recordings from cells with 20 μM microcystin inside the patch pipette. Note the diminished amplitudes of mIPSCs in the CA1 pyramidal cell, but not in the GC, in the presence of microcystin. The *graphs on the right* show cumulative probability distributions of mIPSC peak conductances in the control recordings (*thin lines*) and in recordings with microcystin (20 μM) in the electrode (*thick lines*). In CA1 pyramidal cells (*A*), mIPSCs conductances ($n = 654$ events) were smaller in the presence of microcystin when compared with those recorded in a cell under control conditions ($n = 393$ events), indicating a reduction of mIPSC amplitudes. In the two GCs (*B*), there was no significant difference between mIPSC conductances in control recordings ($n = 324$ events) and those with 20 μM microcystin included in the pipette ($n = 262$ events). *C,* Time course of PKC, PKA, and microcystin effects in CA1 pyramidal cells and GCs. In CA1 pyramidal cells, the gradual diffusion of PKA (*gray circles*) and microcystin (*black circles*) into the cells through the patch electrode caused a significant ($p < 0.05$; *t* test) decrease in mIPSC conductance that reached steady state after 6–7 min of whole-cell recordings. No time-dependent changes were noted with PKC included in the patch pipette. In contrast, in GCs, PKC but not PKA significantly ($p < 0.05$; *t* test) potentiated mIPSCs 9–10 min after the start of the whole-cell recordings. Each point represents the mean conductance (±SD) of >1000 events pooled from $n = 3–5$ cells at each of the indicated time periods.

B   Dentate Gyrus Granule Cells

Control   **Microcystin**

75 pA | 50 ms

C

CA1 Pyramidal Cells   **Dentate Gyrus Granule Cells**

— Control
— PKA
— Microcystin
— PKC

may also alter currents evoked by GABA in CA1 neurons (Stelzer et al., 1988; Chen et al., 1990; Wang et al., 1995).

How does phosphorylation affect the function of synaptic GABARs?

The precise mechanisms whereby phosphorylation of ligand-gated channels alters channel function are not well understood. There might be effects on receptor desensitization, the opening probability of the channels, the interaction between ligand and receptor, or the predominant conductance state to which the channels open. One of the most detailed studies to date on this topic has demonstrated a PKA-induced increase in the probability of channel opening at the peak of currents through homomeric GluR6 channels (Traynelis and Wahl, 1997). The probability of channel opening was intermediate (0.65) under control conditions, but could be increased to 0.85–0.94 when the channels were phosphorylated or reduced to 0.5 when dephosphorylated by the Ca^{2+}/calmodulin-dependent protein phosphatase calcineurin.

Thus, a wide dynamic range may exist for the regulation of the number of channels open at the peak of synaptic responses. In contrast to homomeric GluR6 channels expressed in HEK293 cells, the function of GABARs at CA1 pyramidal cell inhibitory synapses was downregulated by PKA activation. It is tempting to speculate that in these neurons a continuous phosphorylated state may keep synaptic GABARs consistently below their full inhibitory potential. This might be akin to the operation of air brakes, where the compressoractively spends energy to keep the brake pads away from the disks to ensure stopping in the event of a system failure. In the case of GABARs, the steady phosphorylation by PKA may keep the function of the receptors sufficiently low, so that in the event of a cellular metabolic challenge and falling ATP levels, GABAergic inhibition could escape from the suppressing effect of phosphorylation to provide more inhibition for the neuron.

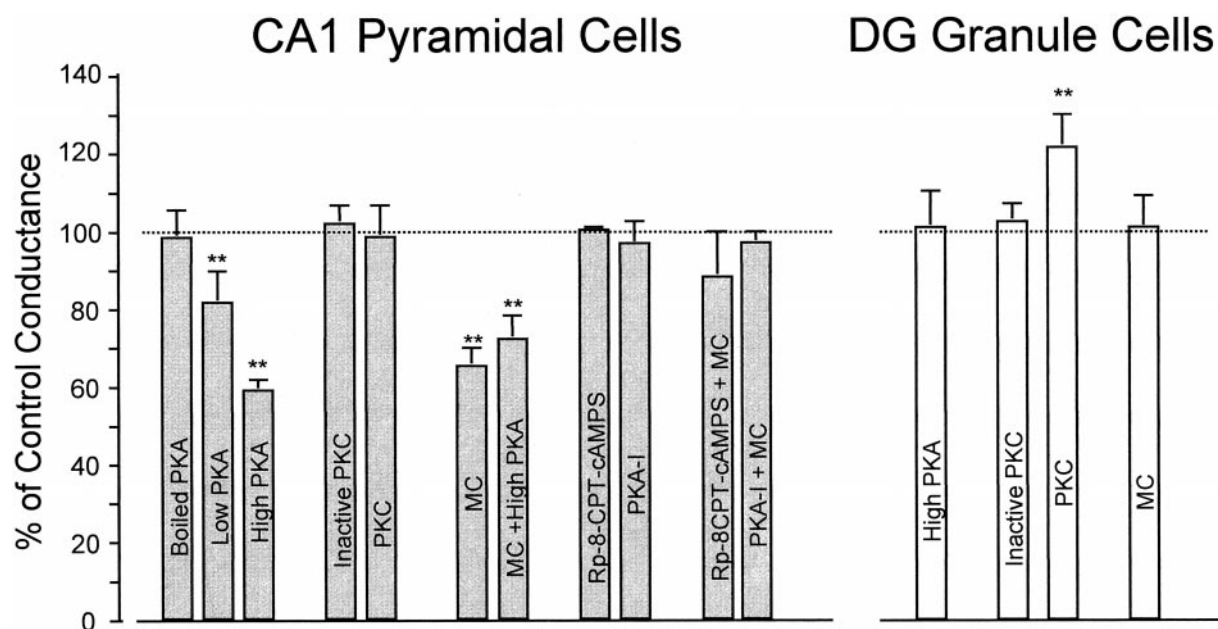It is interesting to note that regardless of an enhancement, as

Figure 5. Modulation of GABAR-mediated mIPSC conductance by intracellular perfusion of protein kinases, protein kinase inhibitors, and protein phosphatase inhibitors. All conductance values were normalized to the control conductance (*dotted line*, 100%) and are represented as percentage. In CA1 neurons (*filled gray bars*) boiled PKA, inactive PKC, and PKA inhibitors alone (intracellular PKA-I, 0.66 μM, and extracellular Rp-8-CPT-cAMP-S, 100 μM) had conductances similar to control. However, PKA (*Low PKA*, 0.6 μg/ml and *High PKA*, 6 μg/ml) and microcystin alone (20 μM) or in combination with PKA (6 μg/ml) showed a significant reduction in mIPSC amplitude. The effects of microcystin were completely abolished by PKA inhibitors (intracellular PKA-I, 0.66 μM, or extracellular Rp-8-CPT-cAMP-S, 100 μM). In GCs (*open bars*), only PKC (6 μgm/ml) induced a significant potentiation of mIPSC conductance. Microcystin, inactive PKC, or PKA (6 μgm/ml) were without effect.

with PKC in the GCs, or a suppression of mIPSCs, as with PKA in CA1 pyramidal cells, the augmented phosphorylation caused an enhanced incidence of biexponentially decaying mIPSCs. In our model, this effect does not need to involve receptor desensitization, but according to a recent study (Jones and Westbrook, 1997), promoting phosphorylation in cultured neurons by inhibiting calcineurin leads to an increased GABA unbinding rate and an enhanced desensitization of fast GABA currents and IPSCs. The kinase responsible for the phosphorylation was not identified in this study, and in contrast to our results, inhibition of PP$_{1/2}$ was without effect on synaptic and evoked GABA currents. Yet, an aspect of our results is clearly consistent with the findings in cultured neurons: a continuous cycle of phosphorylation/dephosphorylation appears to control the function of GABARs.

In conclusion, we have demonstrated that the function of synaptic GABARs in hippocampal CA1 pyramidal cells is under the control of a basal phosphorylation by PKA and that mIPSCs in GCs can be augmented via phosphorylation by PKC. Accordingly, in CA1 pyramidal cells, inhibitory strength will critically depend on the relative intensities of phosphorylation and dephosphorylation. When dephosphorylation outweighs phosphorylation, as may happen during metabolic impairment, this mechanism will ensure a decreased excitability through enhanced GABAR-mediated inhibition.

REFERENCES

Angelotti TP, Uhler MD, Macdonald RL (1993) Enhancement of recombinant gamma-aminobutyric acid type A receptor currents by chronic activation of cAMP-dependent protein kinase. Mol Pharmacol 44:1202–1210.

Aniksztejn L, Sciancalepore M, Ben Ari Y, Cherubini E (1995) Persistent current oscillations produced by activation of metabotropic glutamate receptors in immature rat CA3 hippocampal neurons. J Neurophysiol 73:1422–1429.

Auger C, Marty A (1997) Heterogeneity of functional synaptic parameters among single release sites. Neuron 19:139–150.

Barria A, Muller D, Derkach V, Griffith LC, Soderling TR (1997) Regulatory phosphorylation of AMPA-type glutamate receptors by CaM-KII during long-term potentiation. Science 276:2042–2045.

Browning MD, Bureau M, Dudek EM, Olsen RW (1990) Protein kinase C and cAMP-dependent protein kinase phosphorylate the beta subunit of the purified gamma-aminobutyric acid A receptor. Proc Natl Acad Sci USA 87:1315–1318.

Browning MD, Endo S, Smith GB, Dudek EM, Olsen RW (1993) Phosphorylation of the GABA_A receptor by cAMP-dependent protein kinase and by protein kinase C: analysis of the substrate domain. Neurochem Res 18:95–100.

Capogna M, Gahwiler BH, Thompson SM (1995) Presynaptic enhancement of inhibitory synaptic transmission by protein kinases A and C in the rat hippocampus *in vitro*. J Neurosci 15:1249–1260.

Chang Y, Wang R, Barot S, Weiss DS (1996) Stoichiometry of a recombinant GABAA receptor. J Neurosci 16:5415–5424.

Chen QX, Stelzer A, Kay AR, Wong RKS (1990) GABA_A receptor function is regulated by phosphorylation in acutely dissociated guinea-pig hippocampal neurones. J Physiol (Lond) 420:207–221.

Cheun JE, Yeh HH (1992) Modulation of GABAA receptor-activated current by norepinephrine in cerebellar Purkinje cells. Neuroscience 51:951–960.

Cheun JE, Yeh HH (1996) Noradrenergic potentiation of cerebellar Purkinje cell responses to GABA: cyclic AMP as intracellular intermediary. Neuroscience 74:835–844.

De Koninck Y, Mody I (1994) Noise analysis of miniature IPSCs in adult rat brain slices: properties and modulation of synaptic GABA_A receptor channels. J Neurophysiol 71:1318–1335.

Glitsch M, Llano I, Marty A (1996) Glutamate as a candidate retrograde messenger at interneurone-Purkinje cell synapses of rat cerebellum. J Physiol (Lond) 497:531–537.

Heuschneider G, Schwartz RD (1989) cAMP and forskolin decrease gamma-aminobutyric acid-gated chloride flux in rat brain synaptoneurosomes. Proc Natl Acad Sci USA 86:2938–2942.

Huang RQ, Dillon GH (1998) Maintenance of recombinant type A gamma-aminobutyric acid receptor function: role of protein tyrosine phosphorylation and calcineurin. J Pharmacol Exp Ther 286:243–255.

Jones A, Korpi ER, McKernan RM, Pelz R, Nusser Z, Mäkelä R, Mellor JR, Pollard S, Bahn S, Stephenson FA, Randall AD, Sieghart W, Somogyi P, Smith AJH, Wisden W (1997) Ligand-gated ion channel subunit partnerships: GABA$_A$ receptor α_6 subunit gene inactivation inhibits δ subunit expression. J Neurosci 17:1350–1362.

Jones MV, Westbrook GL (1995) Desensitized states prolong GABA$_A$ channel responses to brief agonist pulses. Neuron 15:181–191.

Jones MV, Westbrook GL (1997) Shaping of IPSCs by endogenous calcineurin activity. J Neurosci 17:7626–7633.

Kano M, Fukunaga K, Konnerth A (1996) Ca^{2+}-induced rebound potentiation of gamma-aminobutyric acid-mediated currents requires activation of Ca^{2+}/calmodulin-dependent kinase II. Proc Natl Acad Sci USA 93:13351–13356.

Kazanietz MG, Areces LB, Bahador A, Mischak H, Goodnight J, ushinski JF, Blumberg PM (1993) Characterization of ligand and substrate specificity for the calcium-dependent and calcium-independent protein kinase C isozymes. Mol Pharmacol 44:298–307.

Kennedy MB (1997) The postsynaptic density at glutamatergic synapses. Trends Neurosci 20:264–268.

Krishek BJ, Xie X, Blackstone C, Huganir RL, Moss SJ, Smart TG (1994) Regulation of GABAA receptor function by protein kinase C phosphorylation. Neuron 12:1081–1095.

Leidenheimer NJ, Browning MD, Harris RA (1991) GABAA receptor phosphorylation: multiple sites, actions and artifacts. Trends Pharmacol Sci 12:84–87.

Leidenheimer NJ, McQuilkin SJ, Hahner LD, Whiting P, Harris RA (1992) Activation of protein kinase C selectively inhibits the gamma-aminobutyric acid A receptor: role of desensitization. Mol Pharmacol 41:1116–1123.

Levitan IB (1994) Modulation of ion channels by protein phosphorylation and dephosphorylation. Annu Rev Physiol 56:193–212.

Lewis CA, Faber DS (1996) Properties of spontaneous inhibitory synaptic currents in cultured rat spinal cord and medullary neurons. J Neurophysiol 76:448–460.

Lin YF, Browning MD, Dudek EM, Macdonald RL (1994) Protein kinase C enhances recombinant bovine alpha 1 beta 1 gamma 2L GABAA receptor whole-cell currents expressed in L929 fibroblasts. Neuron 13:1421–1431.

Macdonald RL, Olsen RW (1994) GABA$_A$ receptor channels. Annu Rev Neurosci 17:569–602.

Machu TK, Firestone JA, Browning MD (1993) Ca^{2+}/calmodulin-dependent protein kinase II and protein kinase C phosphorylate a synthetic peptide corresponding to a sequence that is specific for the gamma$_{2L}$ subunit of the GABA$_A$ receptor. J Neurochem 61:375–377.

McDonald BJ, Moss SJ (1994) Differential phosphorylation of intracellular domains of gamma-aminobutyric acid type A receptor subunits by calcium/calmodulin type 2-dependent protein kinase and cGMP-dependent protein kinase. J Biol Chem 269:18111–18117.

McDonald BJ, Moss SJ (1997) Conserved phosphorylation of the intracellular domains of GABA(A) receptor beta2 and beta3 subunits by cAMP-dependent protein kinase, cGMP-dependent protein kinase protein kinase C and Ca2+/calmodulin type II-dependent protein kinase. Neuropharmacology 36:1377–1385.

McDonald BJ, Amato A, Connolly CN, Benke D, Moss SJ, Smart TG (1998) Adjacent phosphorylation sites on GABAA receptor β subunits determine regulation by cAMP-dependent protein kinase. Nature Neurosci 1:23–28.

McEachern JC, Shaw CA (1996) An alternative to the LTP orthodoxy: a plasticity-pathology continuum model. Brain Res Rev 22:51–92.

McKernan RM, Whiting PJ (1996) Which GABA$_A$-receptor subtypes really occur in the brain? Trends Neurosci 19:139–143.

Morishita W, Kirov SA, Alger BE (1998) Evidence for metabotropic glutamate receptor activation in the induction of depolarization-induced suppression of inhibition in hippocampal CA1. J Neurosci 18:4870–4882.

Moss SJ, Smart TG (1996) Modulation of amino acid-gated ion channels by protein phosphorylation. Int Rev Neurobiol 39:1–52.

Moss SJ, Doherty CA, Huganir RL (1992a) Identification of the cAMP-dependent protein kinase and protein kinase C phosphorylation sites within the major intracellular domains of the beta 1, gamma 2S, and gamma 2L subunits of the gamma-aminobutyric acid type A receptor. J Biol Chem 267:14470–14476.

Moss SJ, Smart TG, Blackstone CD, Huganir RL (1992b) Functional modulation of GABA$_A$ receptors by cAMP-dependent protein phosphorylation. Science 257:661–665.

Moss SJ, Gorrie GH, Amato A, Smart TG (1995) Modulation of GABA$_A$ receptors by tyrosine phosphorylation. Nature 377:344–348.

Nusser Z, Sieghart W, Somogyi P (1998) Segregation of different GABA$_A$ receptors to synaptic and extrasynaptic membranes of cerebellar granule cells. J Neurosci 18:1693–1703.

Otis TS, Mody I (1992) Modulation of decay kinetics and frequency of GABA$_A$ receptor-mediated spontaneous inhibitory postsynaptic currents in hippocampal neurons. Neuroscience 49:13–32.

Pitler TA, Alger BE (1994) Differences between presynaptic and postsynaptic GABA$_B$ mechanisms in rat hippocampal pyramidal cells. J Neurophysiol 72:2317–2327.

Poisbeau P, Williams SR, Mody I (1997) Silent GABA$_A$ synapses during flurazepam withdrawal are region-specific in the hippocampal formation. J Neurosci 17:3467–3475.

Porter NM, Twyman RE, Uhler MD, Macdonald RL (1990) Cyclic AMP-dependent protein kinase decreases GABA$_A$ receptor current in mouse spinal neurons. Neuron 5:789–796.

Raymond LA, Blackstone CD, Huganir RL (1993) Phosphorylation of amino acid neurotransmitter receptors in synaptic plasticity. Trends Neurosci 16:147–153.

Sheng M, Wyszynski M (1997) Ion channel targeting in neurons. BioEssays 19:847–853.

Sieghart W (1995) Structure and pharmacology of gamma-aminobutyric acid A receptor subtypes. Pharmacol Rev 47:181–234.

Sigel E (1995) Functional modulation of ligand-gated GABAA and NMDA receptor channels by phosphorylation. J Recept Signal Transduct Res 15:325–332.

Sigel E, Baur R (1988) Activation of protein kinase C differentially modulates neuronal Na+, Ca2+, and gamma-aminobutyrate type A channels. Proc Natl Acad Sci USA 85:6192–6196.

Sigel E, Baur R, Malherbe P (1991) Activation of protein kinase C results in down-modulation of different recombinant GABAA-channels. FEBS Lett 291:150–152.

Smith RL, Clayton GH, Wilcox CL, Escudero KW, Staley KJ (1995) Differential expression of an inwardly rectifying chloride conductance in rat brain neurons: a potential mechanism for cell-specific modulation of postsynaptic inhibition. J Neurosci 15:4057–4067.

Soderling TR (1995) Calcium-dependent protein kinases in learning and memory. Adv Second Messenger Phosphoprotein Res 30:175–189.

Soltesz I, Mody I (1995) Ca^{2+}-dependent plasticity of miniature inhibitory postsynaptic currents after amputation of dendrites in central neurons. J Neurophysiol 73:1763–1773.

Soltesz I, Smetters DK, Mody I (1995) Tonic inhibition originates from synapses close to the soma. Neuron 14:1273–1283.

Staley KJ, Otis TS, Mody I (1992) Membrane properties of dentate gyrus granule cells: comparison of sharp microelectrode and whole-cell recordings. J Neurophysiol 67:1346–1358.

Stelzer A, Kay AR, Wong RKS (1988) GABA$_A$-receptor function in hippocampal cells is maintained by phosphorylation factors. Science 241:339–341.

Tehrani MH, Hablitz JJ, Barnes EMJ (1989) cAMP increases the rate of GABAA receptor desensitization in chick cortical neurons. Synapse 4:126–131.

Traynelis SF, Wahl P (1997) Control of rat GluR6 glutamate receptor open probability by protein kinase A and calcineurin. J Physiol (Lond) 503:513–531.

Wan Q, Man HY, Braunton J, Wang W, Salter MW, Becker L, Wang YT (1997) Modulation of GABA$_A$ receptor function by tyrosine phosphorylation of β subunits. J Neurosci 17:5062–5069.

Wang LY, Dudek EM, Browning MD, MacDonald JF (1994) Modulation of AMPA/kainate receptors in cultured murine hippocampal neurones by protein kinase C. J Physiol (Lond) 475:431–437.

Wang RA, Cheng G, Kolaj M, Randic M (1995) Alpha-subunit of calcium/calmodulin-dependent protein kinase II enhances gamma-aminobutyric acid and inhibitory synaptic responses of rat neurons in vitro. J Neurophysiol 73:2099–2106.

Weiner JL, Valenzuela CF, Watson PL, Frazier CJ, Dunwiddie TV (1997) Elevation of basal protein kinase C activity increases ethanol sensitivity of GABA(A) receptors in rat hippocampal CA1 pyramidal neurons. J Neurochem 68:1949–1959.

Williams SR, Buhl EH, Mody I (1998) The dynamics of synchronized neurotransmitter release determined from compound spontaneous IPSCs in rat dentate granule neurones *in vitro*. J Physiol (Lond) 510:477–497.